Supplementary Information

Photoactivation of the BLUF Protein PixD Probed by the Site-Specific Incorporation of Fluorotyrosine Residues

Agnieszka A. Gil[‡], Sergey P. Laptenok[§], James N. Iuliano[‡], Andras Lukacs[#], Anil Verma[†], Christopher R. Hall[§], EunBin Yoon[‡], Richard Brust[‡], Gregory M. Greetham[†], Michael Towrie[†], Jarrod B. French[‡,¥], Stephen R. Meech[§,*], Peter J. Tonge[‡,*]

[‡]Department of Chemistry, and [¥]Biochemistry & Cell Biology, Stony Brook University, Stony Brook, New York 11794-3400, USA; [§]School of Chemistry, University of East Anglia, Norwich Research Park, Norwich NR4 7TJ, UK; [#]Department of Biophysics, Medical School, University of Pecs, Pecs, Hungary; [†]Central Laser Facility, Harwell Science and Innovation Campus, Didcot, Oxon OX11 0QX, UK.

*Authors to whom correspondence should be addressed: Email: s.meech@uea.ac.uk (SRM); peter.tonge@stonybrook.edu (PJT)

Contents

Table S1: Primers used for site-directed mutagenesis

	Forward Primer	Reverse Primer
PixD Y8F	GTACCGTTTGATTTTCAGCAGTCAGGGC	GCCCTGACTGCTGAAAATCAAACGGTAC
PixD Y8TAG	GTACCGTTTGATTTAGAGCAGTCAGGGC	GTACCGTTTGATTTAGAGCAGTCAGGGC

Table S2. Quantum yield (QY) of FMN, PixD, and n-FY8 PixDs

	FMN	PixD	3-FY8 PixD	2,3-F_2Y8 PixD	3,5-F_2Y8 PixD	2,3,5-F_3Y8 PixD
QY (%)	21	1-2	3.6	6.6	5.8	5.5

Quantum yield measurements were done as described before [1] using a Quanta F-3029 integrating sphere attached to a Jobin Yvon Nanolog fluorimeter**.**

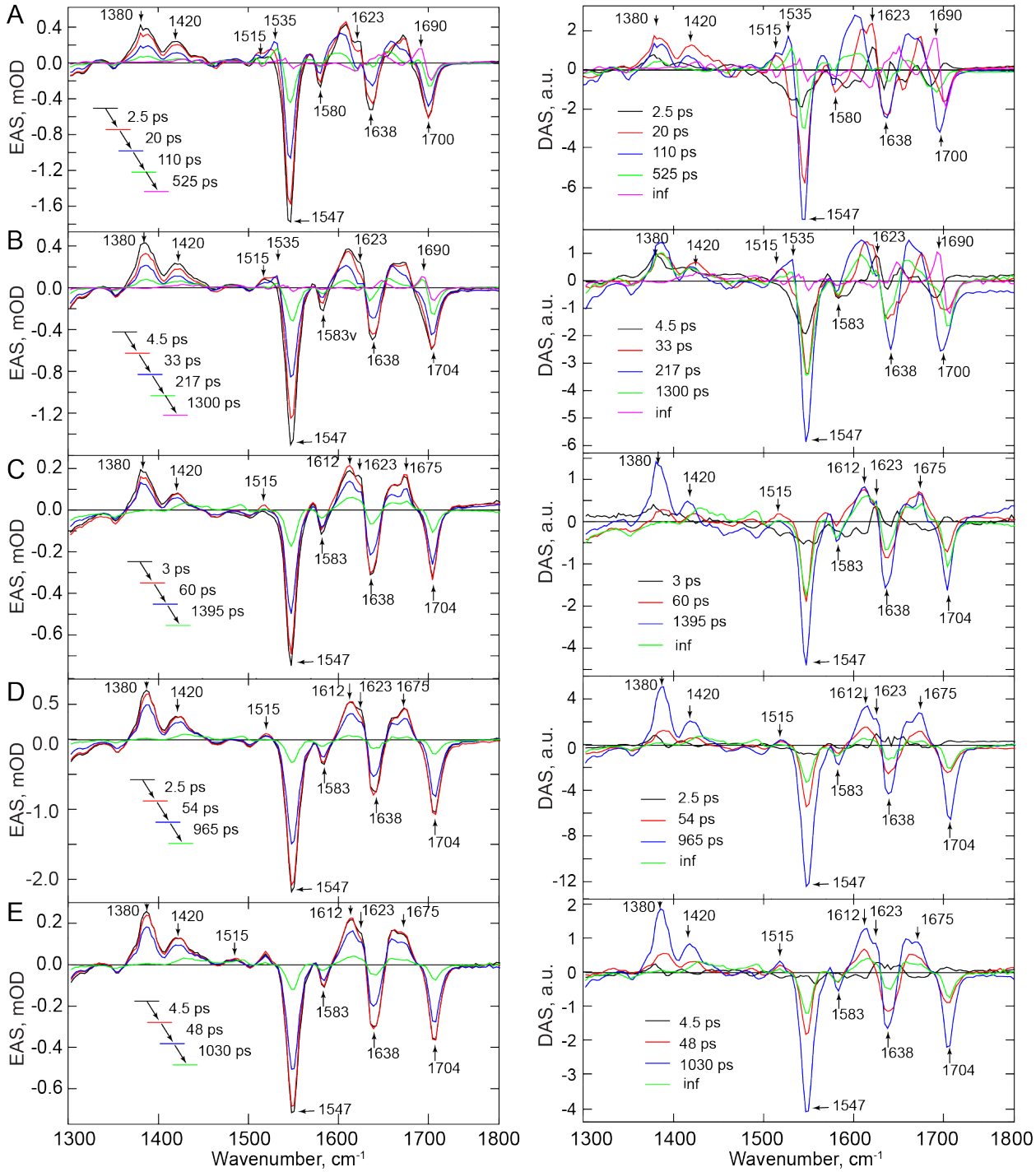

Figure S1: Global analysis of the TRIR data for wild-type PixD and the F-Tyr PixD variants.

EAS are shown in the left column and DAS are shown in the right column. (A) Wild-type, (B) 3-FY8 PixD, (C) 2,3-F_2Y8 PixD, (D) 3,5- F_2Y8 PixD and (E) 2,3,5F_3Y8 PixD.

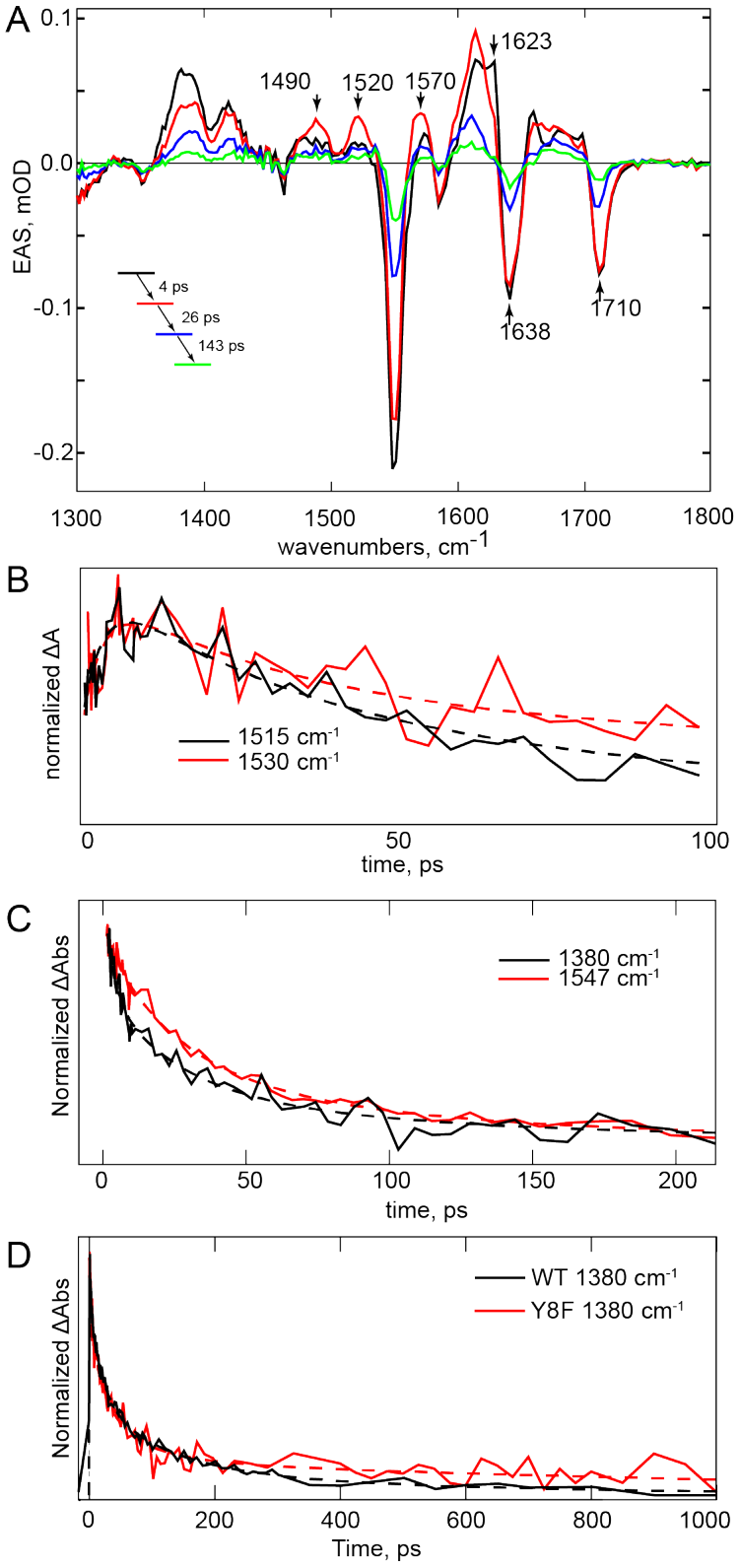

Figure S2: Global analysis of the TRIR data for Y8F PixD.

(A) EAS of Y8F PixD from a global fit of the TRIR data. The time constants needed to adequately describe the data are 4 ps, 26 ps, and 143 ps, with another longer lifetime which is currently not distinguishable. There is no evidence for light state formation in this mutant. (B) Kinetic traces show the change in signal at 1515 and 1530 cm^{-1}. The rise and decay of the signal is consistent with the formation of an FAD radical, however unlike wild-type PixD there is no evidence for the formation of $FADH^{\bullet}$ following $FAD^{\bullet-}$. This is consistent with the hypothesis that W91 acts as the electron donor in the absence of Y8: since W91 cannot donate a proton, proton transfer following the electron transfer is not observed in this mutant. Raw data are shown as solid lines while global fitting results are shown as dashed lines. (C) Kinetic traces of the excited state decay (1380 cm^{-1}) and the ground state recovery (1547 cm^{-1}) showing that the ES decays more rapidly than the ground state recovers, consistent with the formation of an intermediate radical species. (D) Comparison of the excited state decay of wild type and Y8F PixD. Both decay at the same rate.

Figure S3: Mass spectrometric analysis of F-Tyr incorporation into PixD

ESI MS/MS mass spectra were acquired on a Thermo Scientific Orbitrap Fusion Lumos. The mass spectra below are for the peptide that contains residue 8:

LIY*SSQGIPNLQPQDLK

In each case no precursor masses were identified for peptides containing the unmodified Tyr.

(A) 3-FY8 PixD:

The calculated mass $[M+2H]^{2+}$ of the 3-FY8 peptide is 966.45. No unmodified peptide at m/z 957.52 was detected.

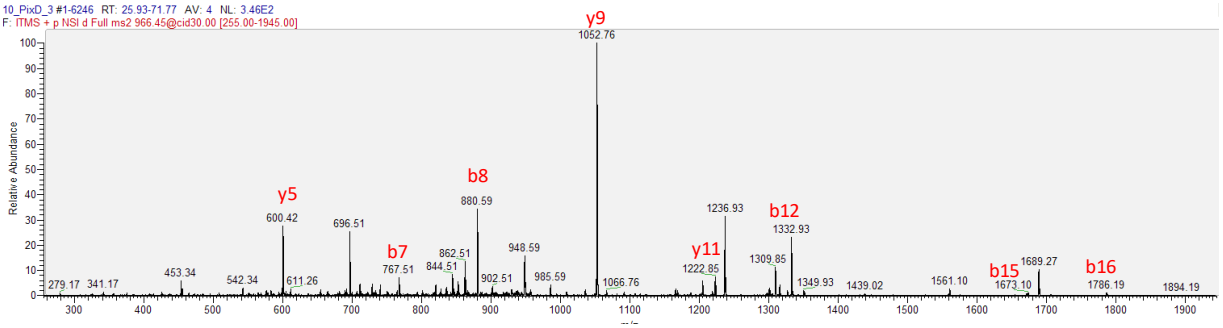

(B) 2,3-F_2Y8 PixD:

The calculated mass $[M+2H]^{2+}$ of the 2,3-F_2Y8 peptide is 975.49. No unmodified peptide at m/z 957.52 was detected.

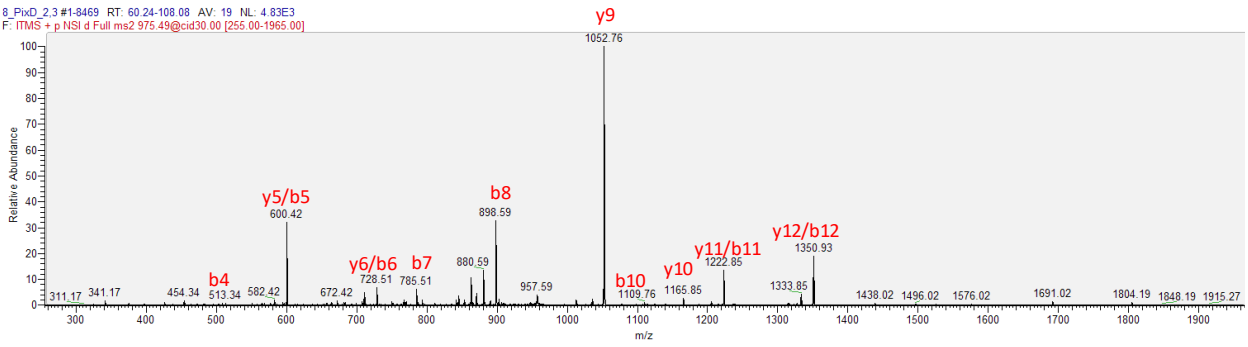

(C) 3,5-F_2Y8 PixD:

The calculated mass $[M+2H]^{2+}$ of the 3,5-F_2Y peptide is 975.49. No unmodified peptide at m/z 957.52 was detected.

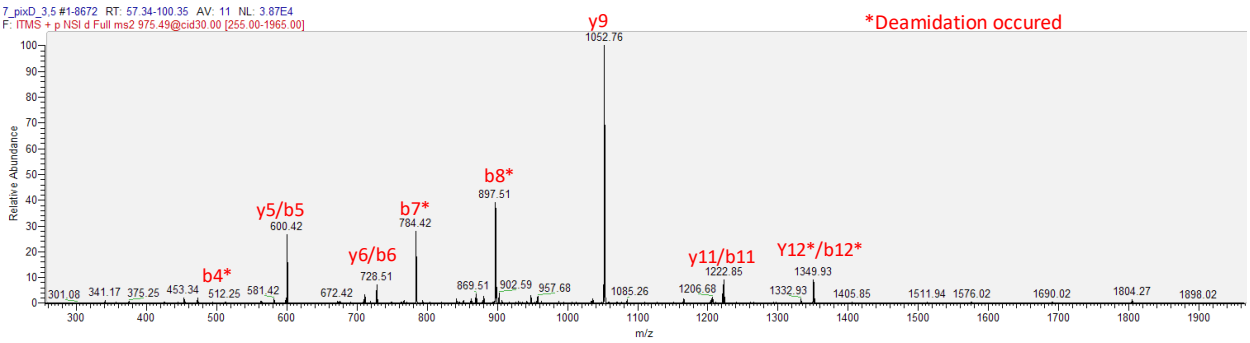

(D) 2,3,5-F_3Y8

The calculated mass $[M+2H]^{2+}$ of the 2,3,5-F_3Y peptide is 984.51. No unmodified peptide at m/z 957.52 was detected.

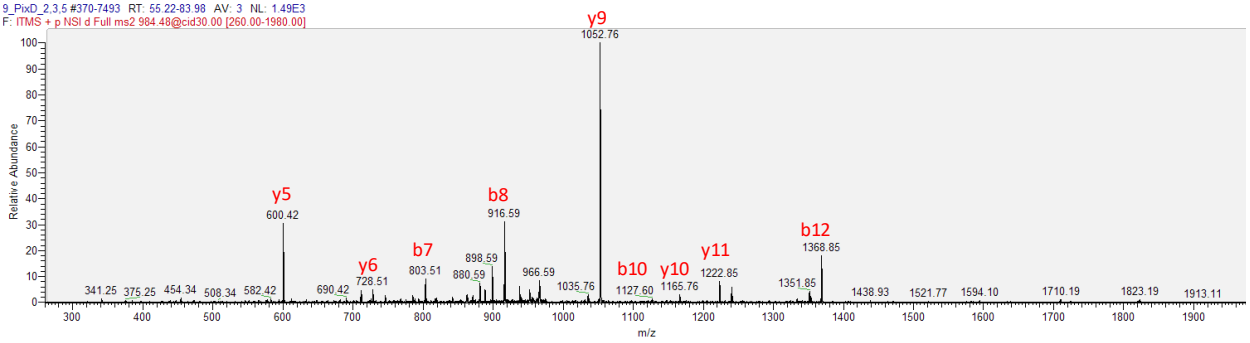

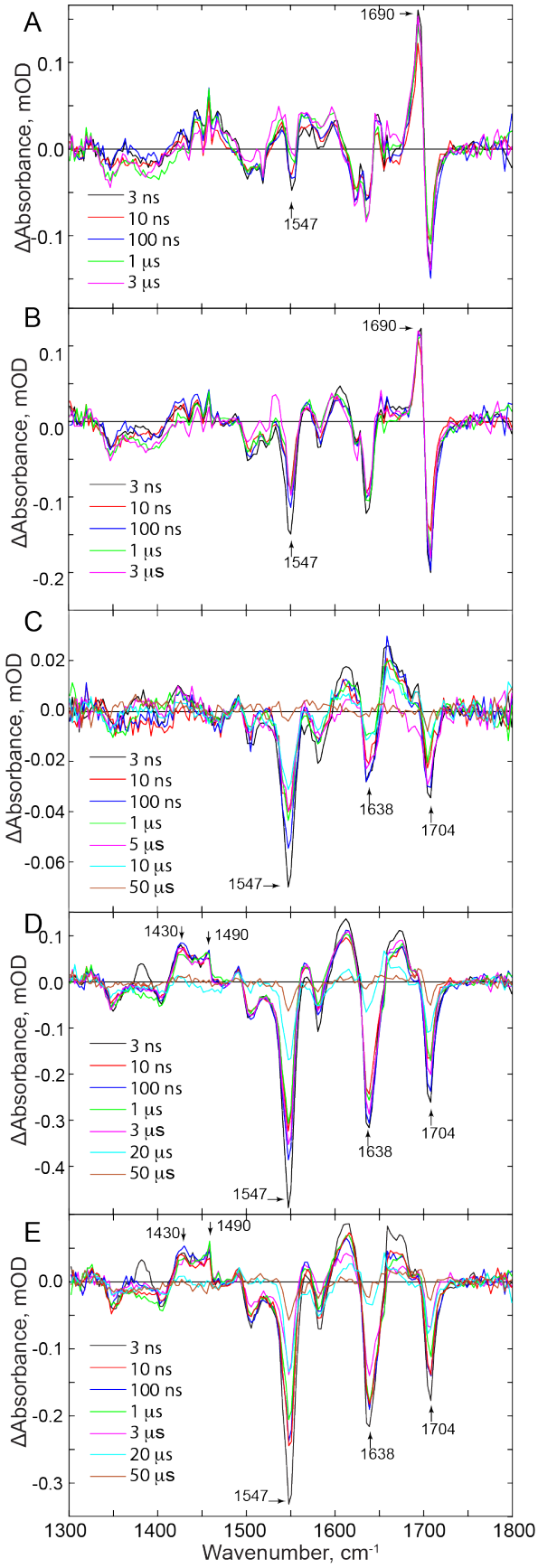
A
B
C
D
E
ΔAbsorbance, mOD
Wavenumber, cm-1
1690
1547
1638
1704
1430
1490
3 ns
10 ns
100 ns
1 µs
3 µs
5 µs
10 µs
20 µs
50 µs

Figure S4: TRMPS Spectra of wild-type and F-Tyr PixDs

(A) wild-type PixD, (B) 3-FY8 PixD, (C) 2,3-F_2Y8 PixD, (D) 3,5-F_2Y8 PixD and (E) 2,3,5-F_3Y8 PixD. There is no further evolution observed of the transient at 1690 cm^{-1} for wild-type and 3-FY8 PixD. For the F_2Y8 and F_3Y8 substituted PixDs, the 1690 cm^{-1} transient is not observed even on the μs timescale. Transients are observed at 1430 and 1490 cm^{-1}, which are indicative of triplet state formation consistent with an increase in lifetime of the excited state.

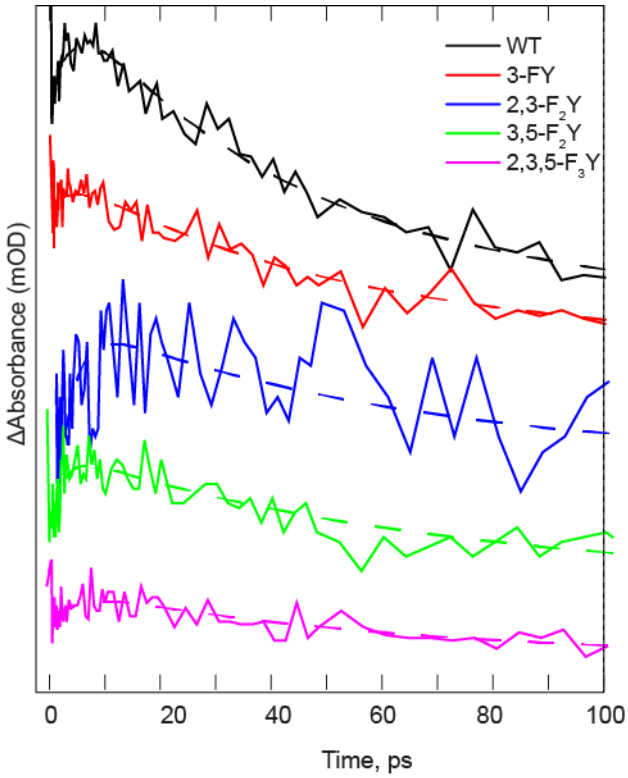

Figure S5. Kinetics of the 1515 cm^{-1} band for wild-type and the F-Tyr PixDs.

Raw data are shown as solid lines while global fitting results are shown as dashed lines.

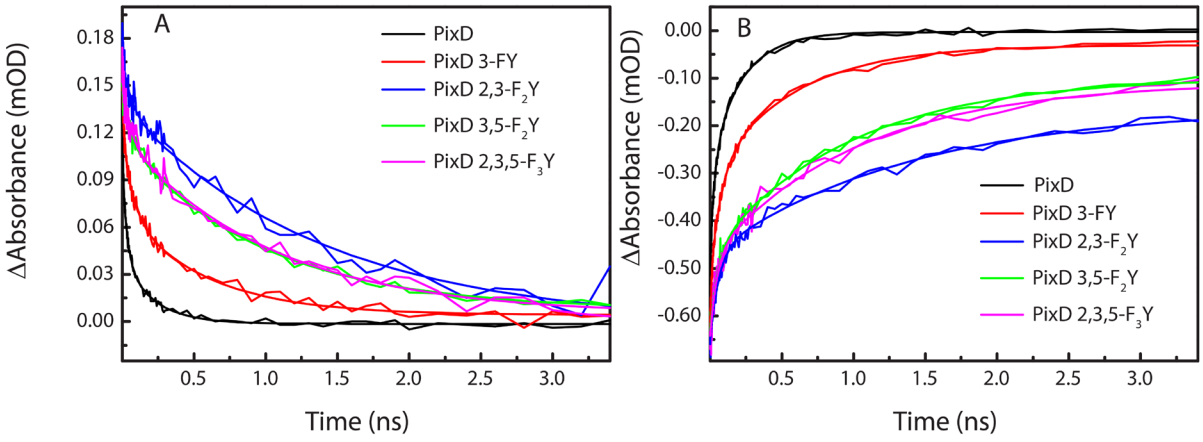

Figure S6: Excited state decay and ground state recovery of wild-type and the F-Tyr PixDs. The smooth solid lines are from a global fit of the data. (A) Excited state decay. (B) Ground state recovery.

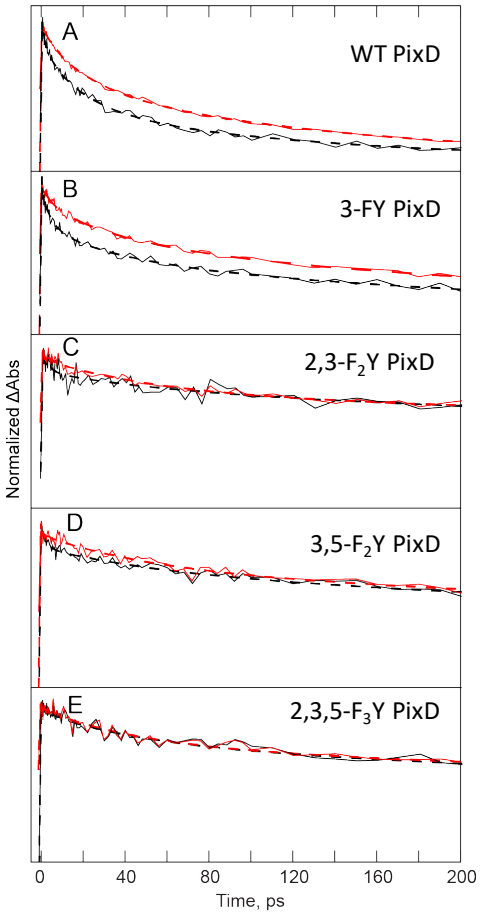

Figure S7: Comparison of excited state decay and ground state recovery for each PixD. The excited state decay is in black and the ground state recovery is in red. (A) wild-type PixD, (B) 3-FY8 PixD, (C) 2,3-F_2Y8 PixD, (D) 3,5-F_2Y8 PixD and (E) 2,3,5-F_3Y8 PixD. Raw data are shown as solid lines while global fitting results are shown as dashed lines.

References

1. Porres, L.; Holland, A.; Palsson, L. O.; Monkman, A. P.; Kemp, C.; Beeby, A., *J Fluoresc* **2006,** *16*, 267.